

Electromagnetically induced transparency in multi-level cascade scheme of cold rubidium atoms

J. Wang,^{1,2} L. B. Kong,^{1,2} K. J. Jiang,^{1,2} K. Li,^{1,2} X. H. Tu,^{1,2} H. W. Xiong,^{1,2} Yifu Zhu,^{3,2} and M. S. Zhan^{1,2}

¹*State Key Laboratory of Magnetic Resonance and Atomic and Molecular Physics,
Wuhan Institute of Physics and Mathematics,
The Chinese Academy of Sciences, Wuhan 430071, P. R. China*

²*Center for Cold Atom Physics, Chinese Academy of Sciences, Wuhan 430071, P. R. China*

³*Department of Physics, Florida International University, Miami, Florida 33199*

(Dated: October 29, 2018)

Abstract

We report an experimental investigation of electromagnetically induced transparency in a multi-level cascade system of cold atoms. The absorption spectral profiles of the probe light in the multi-level cascade system were observed in cold ^{85}Rb atoms confined in a magneto-optical trap, and the dependence of the spectral profile on the intensity of the coupling laser was investigated. The experimental measurements agree with the theoretical calculations based on the density matrix equations of the rubidium cascade system.

PACS: 42.50.-p; 42.50.Gy; 42.50.Hz; 42.65.Ky

Electromagnetically induced transparency (EIT)[1] is a quantum interference effect that permits propagation of light through an opaque atomic medium without attenuation, it was first proposed in 1989 [2] and experimentally verified in 1991 [3]. Since then, theoretical and experimental studies of EIT have attracted great attentions due to their potential applications in many fields, such as low light nonlinear optics [4], quantum information [5], atomic frequency standard [6], and so on. Early studies were carried out with hot atoms in vapor cells. In the hot atomic medium, the interaction time between the atoms and the laser fields is short which leads to the transient broadening. Also, the collisions in the hot atomic medium may severely shorten the coherence decay time. Recently, many groups explored the EIT phenomena using the laser cooled atoms. There are several advantages in the cold atoms [7]. Firstly, because of the low temperature of the cold atoms, the Doppler broadening effect is effectively minimized, which renders it possible to explore EIT-type nonlinear optical phenomena involving odd number of photons. Secondly, the lower collision rates in the cold atomic sample reduce the decoherence rate.

Early experimental studies of EIT in the cold atoms were mainly carried out in rubidium atoms [8, 9, 10]. Subsequently, the EIT based nonlinear optical phenomena were studied [4, 11], which led to the recent experiments on the resonant nonlinear optics at low light intensity. A very steep slope of refractive index and the extremely low group velocity of probe light have been obtained in the cold EIT mediums [12], which have been used to demonstrate light storage and recall based on the coherent excitation transfer between the photons and the atoms [13]. Recently, electromagnetically induced grating (EIG) [14, 15] was realized in the cold atoms. Jason et al. experimentally compared the EIT phenomena between the hot atoms and the cold atoms [16], and Ahufinger et al. compared the EIT phenomena between the cold atoms above and below the transition temperature for Bose-Einstein condensation [17]. These studies on EIT and the related phenomena in the cold atoms provided intensive understanding of the atomic coherence and interference in the fundamental interaction between the light field and the atoms [18, 19, 20, 21, 22, 23].

EIT in the simple three-level system have been extensively studied, but EIT in the multi-level cascade systems and their possible applications have not been fully explored. Although essential physics about EIT has been understood well from the studies of the simple three-level systems, there are several interesting features in the complicated multi-level systems. First, it is possible to create multiple EIT windows in such systems, which will simultane-

ously support slow group velocities for two or more probe pulses at different frequencies. As discussed in ref [24], two light fields propagating with slow group velocities have advantage to efficiently produce the quantum entanglement. The complicated multi-level systems supporting slow group velocities for multiple light fields may provide such interesting possibilities. Second, multi-level EIT systems may be useful for nonlinear light generation processes [19, 25]. In the simple three-level EIT system, degenerate four-wave mixing can be enhanced due to the reduction of the light absorption near the EIT window. Since the complicated multi-level systems exhibit multiple EIT windows, the non-degenerate four-wave mixing processes may be efficiently produced by choosing the pump fields with frequencies near the multiple EIT windows.

Recently, McGloin et al [26] theoretically studied an N-level EIT system with several coupling fields and found that the spectral profiles were quite different from that in the simple three-level EIT systems. The cascade EIT system was studied in a vapor cell at room temperatures [27, 28] and the EIT for resonant two-photon transitions in rubidium atomic vapors was reported by Xu et al [29]. In our previous work, the multi-window EIT produced by bichromatic coupling fields was demonstrated [30]. Here, we report an experimental study of EIT in a multi-level cascade system in cold ^{85}Rb atoms. We apply an intense coupling field that is nearly resonant with the three sets of transitions among the $5P_{3/2}$ and $5D_{5/2}$ levels. We investigate the probe absorption spectra with multiple spectral peaks and the dependence of the probe absorption profiles on the intensities of the coupling laser. Our experimental measurements agree with the theoretical calculations.

We consider cascade EIT system shown in Fig. 1(a), an intense coupling laser with frequency ω_c drives the transition $|2\rangle \rightarrow |3\rangle$, and a weak probe laser with frequency ω_p drives the transition $|1\rangle \rightarrow |2\rangle$. Δ_c and Δ_p are frequency detuning of the coupling laser and the probe laser, respectively. EIT occurs when the coupling and the probe laser frequency satisfy the two-photon resonant condition: $\Delta_c = \Delta_p$. Scanning the probe laser around the transition $|1\rangle \rightarrow |2\rangle$, a typical double-peaked EIT spectrum will appear as shown in Ref. [31]. However, for ^{85}Rb atoms, the upper excited state $|3\rangle$ ($5D_{5/2}$) consists of three closely-spaced hyperfine levels $F'' = 2, 3$, and 4 as shown in Fig. 1(b). The coupling laser will directly drive three sets of transitions $5P_{3/2}, F' = 3 \rightarrow 5D_{5/2}, F'' = 4$, $5P_{3/2}, F' = 3 \rightarrow 5D_{5/2}, F'' = 3$, and $5P_{3/2}, F' = 3 \rightarrow 5D_{5/2}, F'' = 2$. We define the coupling and probe laser detuning as $\Delta_c = \omega_c - \omega_0$ and $\Delta_p = \omega_p - \omega_{21}$ respectively (ω_0 is the resonant frequency of the transition $5P_{3/2}$,

$F = 3 \rightarrow 5D_{5/2}, F'' = 3$, ω_{21} is the resonant frequency of the transition $5S_{1/2}, F = 3 \rightarrow 5P_{3/2}, F' = 3$). Because the frequency separations of the hyperfine components of $5D_{5/2}$ are quite small (less than 10 MHz [32]), the ^{85}Rb cascade system will exhibit clear multi-window EIT effect even with a moderately intense coupling laser. The probe absorption spectrum will display a line profile with multiple peaks corresponding to the multiple dressed states generated by the coupling between the three sets of transitions, and the multiple transparent windows with minimum absorption locate between the peaks. The corresponding probe dispersion will exhibit a line profile with normal steep slopes at several frequencies near the multiple transparent windows. Therefore, the multi-level cascade system supports slow group velocities simultaneously for light pulses at different frequencies.

We carry out a theoretical calculation of a five-level system as shown in Fig.1 (a). The Rabi frequencies for the probe and coupling laser are defined as $2\Omega_p = 2\mu_{21}E_p/\hbar$ and $2\Omega_c = 2\mu_{32}E_c/\hbar$. The master equation is derived under the dipole interaction and the rotating-wave approximation as

$$\dot{\rho} = -\frac{i}{\hbar}[H, \rho] + \gamma_{21}L_{21}\rho + \gamma_{32}L_{32}\rho + \gamma_{42}L_{42}\rho + \gamma_{52}L_{52}\rho \quad (1)$$

Where the system Hamiltonian is written in the form

$$H = H_0 + H_I \quad (2)$$

H_0 is the free Hamiltonian and H_I is the interaction Hamiltonian,

$$H_0 = -\hbar\Delta_p\sigma_{22} - \hbar(\Delta_p + \Delta_c + \delta_1)\sigma_{44} - \hbar(\Delta_p + \Delta_c)\sigma_{33} - \hbar(\Delta_p + \Delta_c - \delta_2)\sigma_{55} \quad (3)$$

$$H_I = -\hbar\Omega_p\sigma_{21} - \hbar a_{32}\Omega_c\sigma_{32} - \hbar a_{42}\Omega_c\sigma_{42} - \hbar a_{52}\Omega_c\sigma_{52} + H.c. \quad (4)$$

with $\delta_1 = \omega_{34} = 9$ MHz, $\delta_2 = \omega_{53} = 7.6$ MHz. $\sigma_{ij} = |i\rangle\langle j|$ ($i, j = 1 \sim 5$) are the population operators when $i = j$ and dipole operators when $i \neq j$. a_{32} , a_{42} and a_{52} are the relative strengths of the three transitions from the three hyperfine sublevels $|3\rangle$, $|4\rangle$ and $|5\rangle$ ($F'' = 3, 4, 2$) to the state $|2\rangle$ ($F' = 3$), and $a_{32} : a_{42} : a_{52} \approx 1 : 1.46 : 0.6$. γ_{ij} denotes the spontaneous emission rates from level i to level j , here $\gamma_{32} = \gamma_{42} = \gamma_{52} = \gamma = 0.97$ MHz,

$L_{ij}\rho$ describes the atomic decay from level i to level j and takes the form

$$L_{ij}\rho = \frac{1}{2}(2\sigma_{ji}\rho\sigma_{ij} - \sigma_{ij}\sigma_{ji}\rho - \rho\sigma_{ij}\sigma_{ji}) \quad (5)$$

We numerically solve the density matrix equations of the five-level system in the steady state. The calculated probe absorption $[\text{Im}(\rho_{21})]$ and probe dispersion $[\text{Re}(\rho_{21})]$ versus the probe detuning Δ_p are plotted in Fig. 2. The absorption spectrum exhibits three dips, and the corresponding dispersion profile exhibits three steep normal slopes, which should be useful for supporting slow light pulses at different frequencies. Fig. 2(a), (b) and (c) show the calculated probe absorption and dispersion profiles for the coupling Rabi frequencies $\Omega_c = 4\gamma$, 7γ , and 12γ respectively, where the coupling detuning $\Delta_c = -9\gamma$. We find that the frequency separations between the neighboring absorption peaks are proportional to the coupling intensity, the width and the location of the EIT windows can be controlled by the intensity and the frequency detuning of the coupling laser. As one example, the multi-level EIT system may be used to produce simultaneously two slow photons at different frequencies, which may be used to generate photon entanglement effectively [24].

Our experiment is carried out in a rubidium atom MOT [33], and the experimental setup is briefly shown in Fig.3. The cooling and trapping beam(780 nm) is supplied by a 500 mW diode laser system(TOPTICA TA100), its frequency is stabilized by the saturated absorption spectra method, and its linewidth is less than 1 MHz. The frequency of the trapping laser is red-detuned about 12 MHz to the $F = 3 \rightarrow F' = 4$ transition by using an acousto-optic modulator(AOM). The repumping laser (780 nm) from a 50 mW diode laser(TOPTICA DL100) is tuned to $F = 2 \rightarrow F'$ transition of ^{85}Rb D_2 line. We get a near spherical atom cloud with the diameter of 3 mm in the MOT, containing about 5×10^7 atoms, and the temperature of atom cloud is about 100 μK . The coupling beam for EIT is taken from a Ti:sapphire laser (Coherent MBR110) and the beam diameter is 3 mm. The transverse modes of the above lasers are filtered to the fundamental Gaussian mode via single mode polarization maintenance fibers. Another 50 mW diode laser (TOPTICA DL100) supplies weak probe beam, the laser beam diameter is 1 mm and laser power is 1 μW . Both the coupling and the probe beams are linearly polarized. They pass through the atom cloud in opposite directions and overlap in the path via polarization beam splitter (PBS). A photodiode (PD) is used to detect the probe light, and a digital oscilloscope (Tektronix TDS 220) is adopted to monitor and record the probe signals.

In order to avoid the influence of the MOT laser, we design a time sequence using AOMs and functional generators (SRS DS345). The experiment is running at a repetition of 10 Hz. In every 100 ms period, the cooling and trapping process last for 97.5 ms, and the scanning of the probe absorption remains 2.5 ms. We find that there is no obvious difference in the absorption spectra between the situations of MOT on and MOT off, so in most time our experiment is carried out with the MOT on.

We tune the coupling laser nearly resonant to the transition $5P_{3/2}, F' = 3 \rightarrow 5D_{5/2}, F'' = 2$, and the probe laser is scanned across the transition $5S_{1/2}, F = 3 \rightarrow 5P_{3/2}, F' = 2, 3, 4$. When the coupling beam is blocked, we get absorption spectrum of cold ^{85}Rb atoms as shown by dashed line in Fig. 4, and the linewidth of each absorption peak is broader than the natural linewidth of the corresponding transition. This is caused mainly by Zeeman shift because we do not shut off the MOT magnetic field during the period of data acquiring. The solid line in Fig. 4 shows the absorption spectrum of the probe laser with coupling laser on, the absorption peak is broadened and is split into several peaks, and the dips between the absorption peaks are probe transparencies induced by the coupling laser field. The system is quite different from that described in Ref. [24], here we select $F = 3 \rightarrow F' = 3$ as the probe transition, and the possible coupling transition for observation of the cascade EIT are $F' = 3 \rightarrow F'' = 2, 3$ and 4. The space between the sublevels $F'' = 2$ and $F'' = 3$ is 7.6 MHz, and the space between sublevels $F'' = 3$ and $F'' = 4$ is 9.0 MHz. When the coupling laser is near resonance with the $F' = 3 \rightarrow F'' = 3$ transition, because of the small spaces of $5D_{5/2}$ sublevels, one coupling laser tuned to $5P_{3/2}, F' = 3 \rightarrow 5D_{5/2}, F''$ transition can be regarded as several coupling fields, but with different detuning for different F'' . The reason of choosing such a level configuration is that with the smaller separation of sublevels of $5D_{5/2}$ and the smaller Zeeman shift of $5P_{3/2}, F = 2$ sublevel, we expect to obtain more EIT dips with high resolution in cold atoms.

We tune coupling laser nearly resonant to the transition $5P_{3/2}, F' = 3 \rightarrow 5D_{5/2}, F'' = 3$, and investigate the dependence of probe spectra on the coupling intensities. The experimental results with $\Delta_c = -2$ MHz are shown in Fig. 5. Figure 5(a) is the probe spectrum with the coupling Rabi frequency $\Omega_c = 2$ MHz, the solid curve is the experimental data, and the dashed line is the calculated results with the spectral broadened arbitrarily to fit the experimental results. Figures 5(b), 5(c), and 5(d) are for $\Omega_c = 4, 6$, and 9 MHz respectively. With the higher coupling intensity, we obtain the deeper and the broader transparency dips.

We perform an experimental study of multi-level cascade type electromagnetically induced transparency in cold ^{85}Rb atoms confined in a MOT. We obtain the unusual absorption profiles with multi-windows EIT. It is possible to realize slow photons with multiple different frequencies synchronously in such a multi-level cascade EIT system and to improve the controllability of quantum information based on EIT. We investigate the dependence of the probe absorption spectra on the coupling intensity. The calculations based on density matrix equations agree with the experimental results.

Support from the National Natural Science Foundation of China under Grant Nos. 10104018 and 10374120 is acknowledged. YZ acknowledges support from the National Science Foundation (Grant No. 001432).

-
- [1] M. D. Lukin, A. Imamoglu, *Nature* 413 (2001) 273.
 - [2] A. Imamoglu and S. E. Harris, *Opt. Lett.* 14 (1989) 1344.
 - [3] K. J. Boller, A. Imamoglu, S. E. Harris, *Phys. Rev. Lett.* 66 (1991) 2593.
 - [4] S. E. Harris, L. V. Hau, *Phys. Rev. Lett.* 82 (1999) 4611.
 - [5] M. Paternostro, M. S. Kim, B. S. Ham, *Phys. Rev. A* 67 (2003) 023811.
 - [6] S. Knappe, J. Kitching, L. Hollberg, *Appl. Phys. Lett.* 81 (2002) 553.
 - [7] Y. C. Chen, C. W. Lin, I. A. Yu, *Phys. Rev. A* 61 (2000) 053805.
 - [8] T. van der Veldt, J. F. Roch, P. Grelu, P. Grangier, *Opt. Commun.* 137 (1997) 420.
 - [9] S. A. Hopkins, E. Usadi, H. X. Chen, A. V. Durrant, *Opt. Commun.* 138 (1997) 185.
 - [10] H. X. Chen, A. V. Durrant, J. P. Marangos, J. A. Vaccaro, *Phys. Rev. A* 58 (1998) 1545.
 - [11] F. S. Cataliotti, C. Fort, T. W. Hänsch, M. Inguscio, M. Prevedelli, *Phys. Rev. A* 56 (1997) 2221.
 - [12] L. Vestergaard Hau, S.E. Harris, Z. Dutton, C.H. Behroozi, *Nature* 397 (1999) 594.
 - [13] C. Liu, Z. Dutton, C.H. Behroozi, L. Vestergaard Hau, *Nature* 409 (2001) 490.
 - [14] Masaharu Mitsunaga, Nobuyuki Imoto, *Phys. Rev. A* 59 (1999) 4773.
 - [15] G. C. Cardoso, J. W. R. Tabosa, *Phys. Rev. A* 65 (2002) 033803.
 - [16] Jason J. Clarke, William A. van Wijngaarden, *Phys. Rev. A* 64 (2001) 023818.
 - [17] V. Ahufinger, R. Corbalán, F. Cataliotti, S. Burger, F. Minardi, C. Fort, *Opt. Commun.* 211 (2002) 159.

- [18] M. Yan, E. G. Rickey, Y. Zhu, Phys. Rev. A 64 (2001) 013412; *ibid*, 043807.
- [19] Y. Wu, J. Saldana, and Yifu Zhu, Phys Rev. A 67, (2003) 013811.
- [20] Y. C. Chen, Y. A. Liao, H. Y. Chiu, J. J. Su, I. A. Yu, Phys. Rev. A 64 (2001) 053806.
- [21] D. C. Roberts, T. Gasenzer, and K. Burnett, Phys. Rev. A 66 (2002) 023801.
- [22] L. Deng, M. G. Payne, E. W. Hagley, Opt. Commun. 198 (2001) 129.
- [23] Özgür E. Müstecapoglu, L. You, Opt. Commun. 193 (2002) 301.
- [24] M. D. Lukin, A. Imamoglu, Phys. Rev. Lett. 84 (2000) 1419.
- [25] L. Deng, M. Kozuma, E. W. Hagley, and M. G. Payne, Phys. Rev. Lett. 88 (2002) 143902.
- [26] D. McGloin, D. J. Fulton, M. H. Dunn, Opt. Commun. 190 (2001) 221.
- [27] R. R. Moseley, S. Shepherd. D. J. Fulton, B. D. Sinclair, M. H. Dunn, Opt. Commun. 119 (1995) 61.
- [28] S. Jin, Y. Li, M. Xiao, Opt. Commun. 119 (1995) 90.
- [29] J. H. Xu, G. C. La Rocca, F. Bassani, D. Wang, J.Y. Gao, Opt. Commun. 216 (2003) 157.
- [30] J. Wang, Yifu Zhu, K. J. Jiang, M. S. Zhan, Phys. Rev. A 68 (2003) 063810.
- [31] J. Gea-Banacloche, Y. Li, S. Jin, M. Xiao, Phys. Rev. A 51 (1995) 576.
- [32] F. Nez, F. Biraben, R. Felder, Y. Millerieux, Opt. Commun. 102 (1993) 432.
- [33] J. Wang, X. J. Liu, J. M. Li, H. T. Zhao, K. J. Jiang, M. S. Zhan, Acta. Opt. Sin. 20 (2000) 862 (in Chinese).

Figurecaptions

Fig. 1 Level configuration of the cascade type electromagnetically induced transparency, (a) is schematic diagram; (b) is energy levels of cold ^{85}Rb atoms.

Fig.2 The calculated probe absorption spectra of multi-level cascade EIT in cold ^{85}Rb atoms. The probe laser scans across the transition $5S_{1/2}, F = 3 \rightarrow 5P_{3/2}, F' = 3, \Delta_c = -9\gamma$ ($\gamma = 0.97$ MHz). (a), (b) and (c) are for $\Omega_c = 4\gamma, 7\gamma$, and 12γ respectively. The dashed lines are dispersion profiles.

Fig. 3 The experimental setup for electromagnetically induced transparency in cold atoms confined in a magneto-optical trap. PBS: polarizing beam splitter; PD: photodiode; L: lens; BS: beam splitter; M: mirror; AOM: acousto-optic modulator.

Fig. 4 Absorption spectra of the multi-level cascade type EIT in cold ^{85}Rb atoms with

$\Omega_c = 4$ MHz and $\Delta_c = -2$ MHz, the probe laser scans across the transitions $5S_{1/2}, F = 3 \rightarrow 5P_{3/2}, F' = 2, 3, 4$. The dashed line is the absorption spectrum without the coupling laser, and the solid line is that with the coupling laser on. The linewidth of the absorption peak is broadened by Zeeman shifts.

Fig. 5 The multi-level cascade type EIT spectra of ^{85}Rb with the different coupling laser intensities with $\Delta_c = -2$ MHz, the probe laser scans across the transitions $5S_{1/2}, F = 3 \rightarrow 5P_{3/2}, F' = 3$. (a), (b), (c), and (d) are $\Omega_c = 2, 4, 6$, and 9 MHz respectively. The solid curves are the experimental data and the dashed lines are the calculated results with the spectral broadened arbitrarily to fit the experimental linewidth.

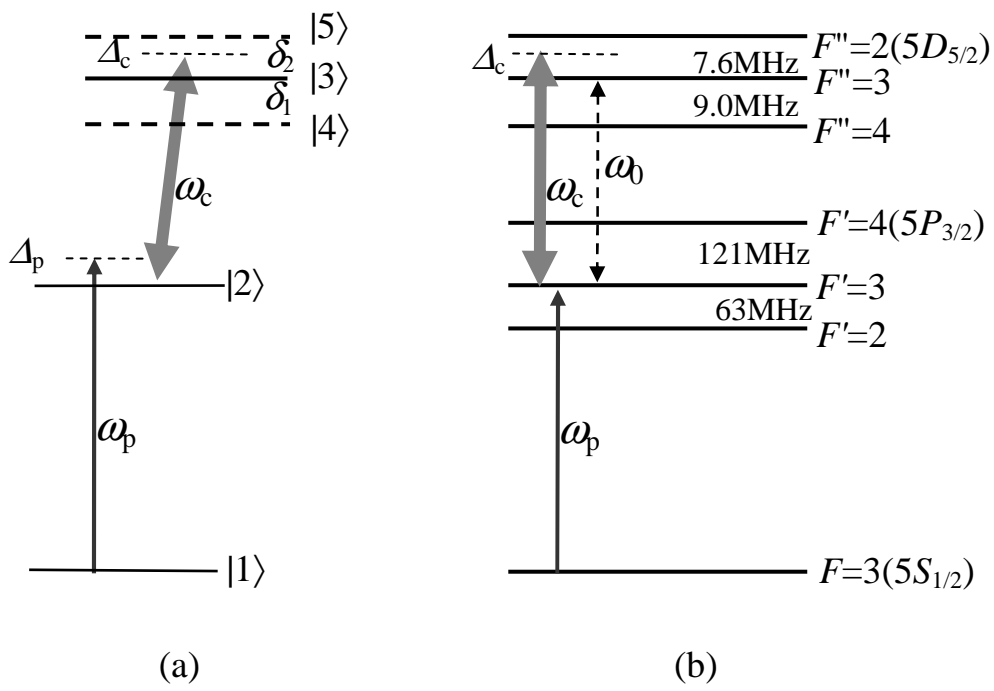
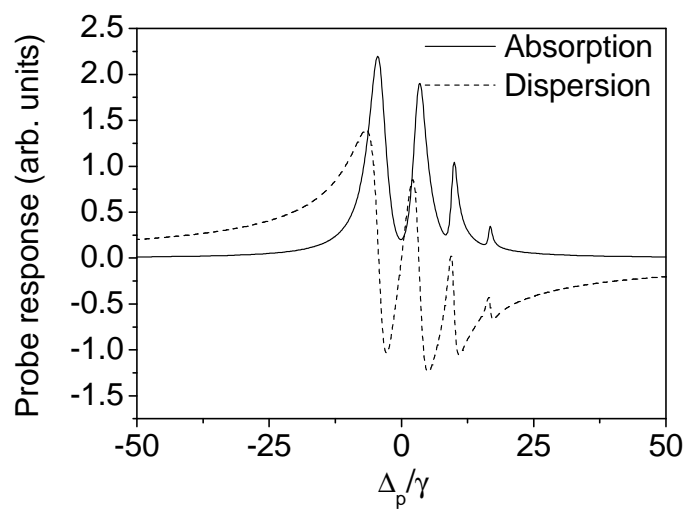
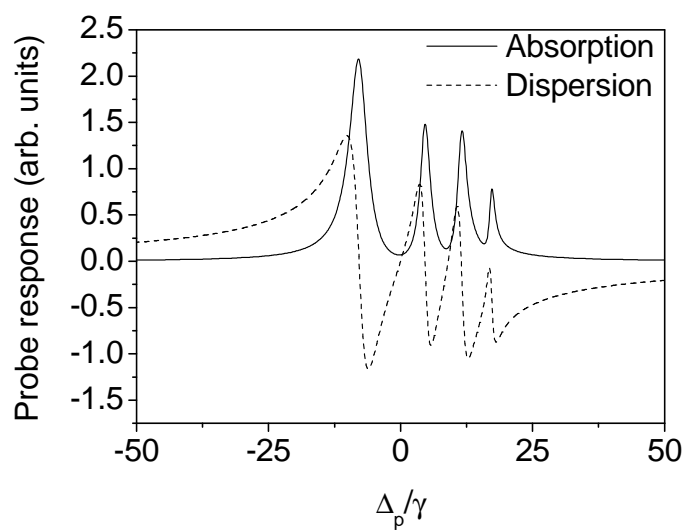


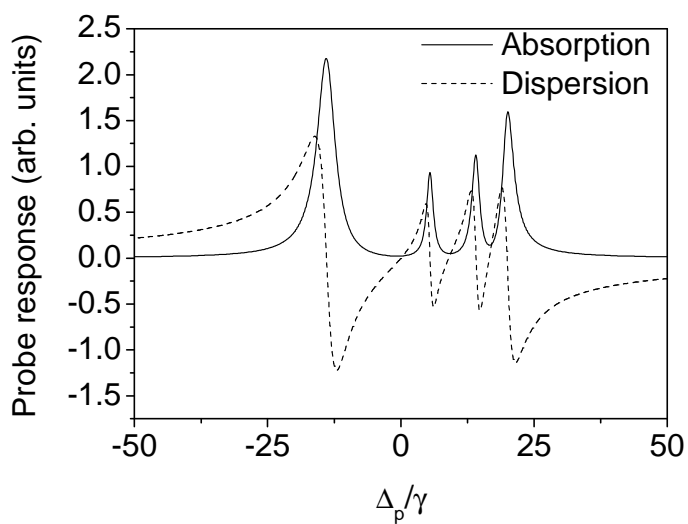
Fig. 1 (J. Wang et al)



(a)



(b)



(c)

Fig.2 (J. Wang et al)

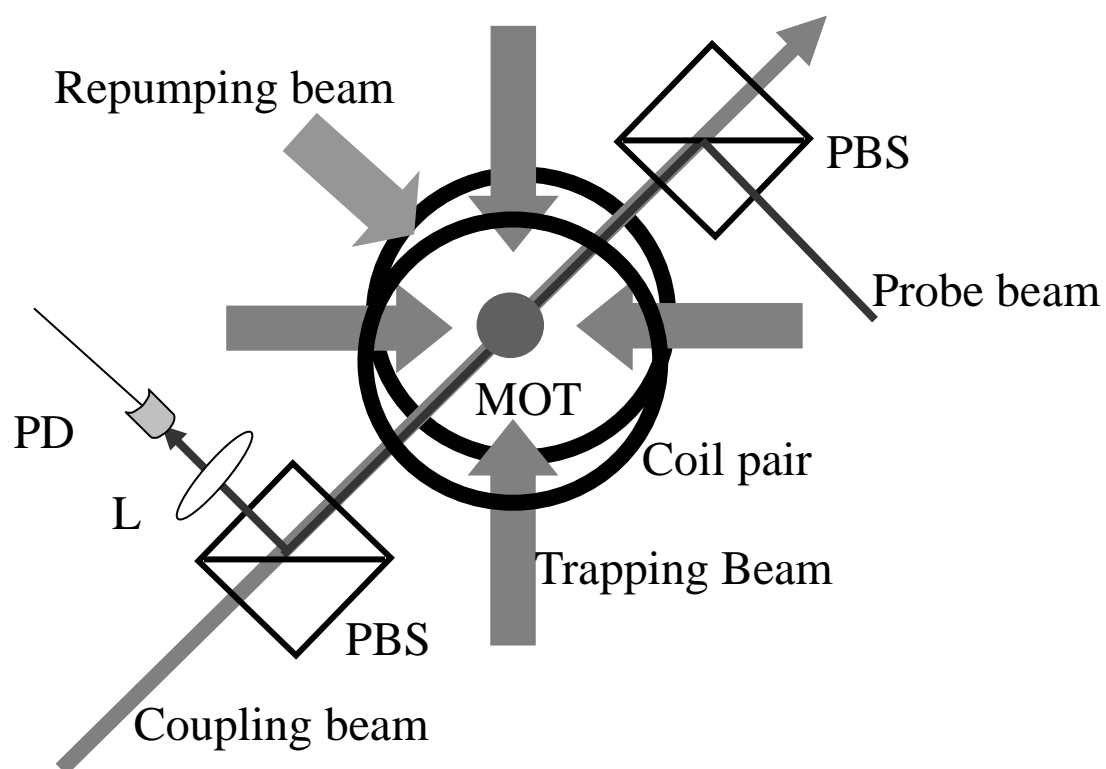


Fig. 3 (J. Wang et al)

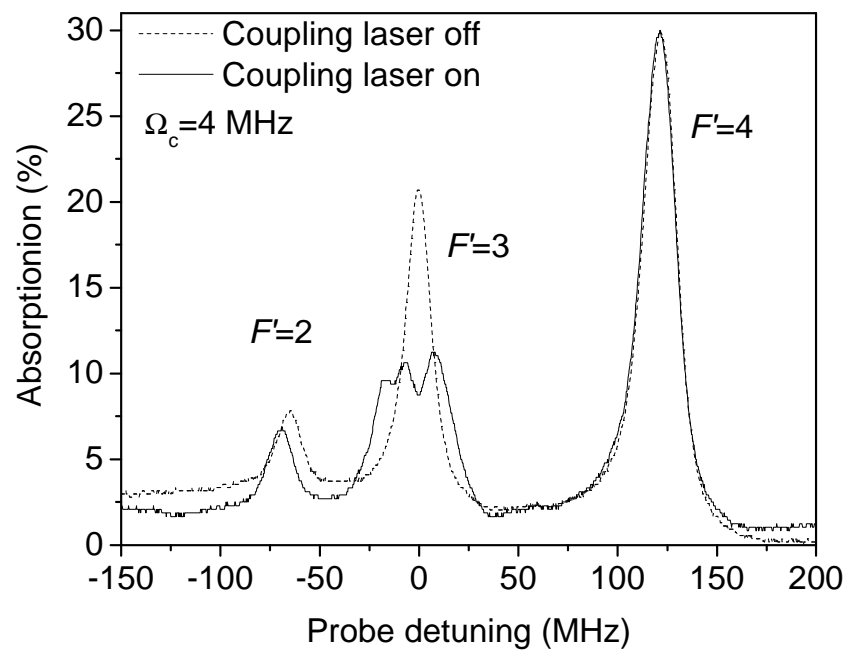


Fig. 4 (J. Wang et al)

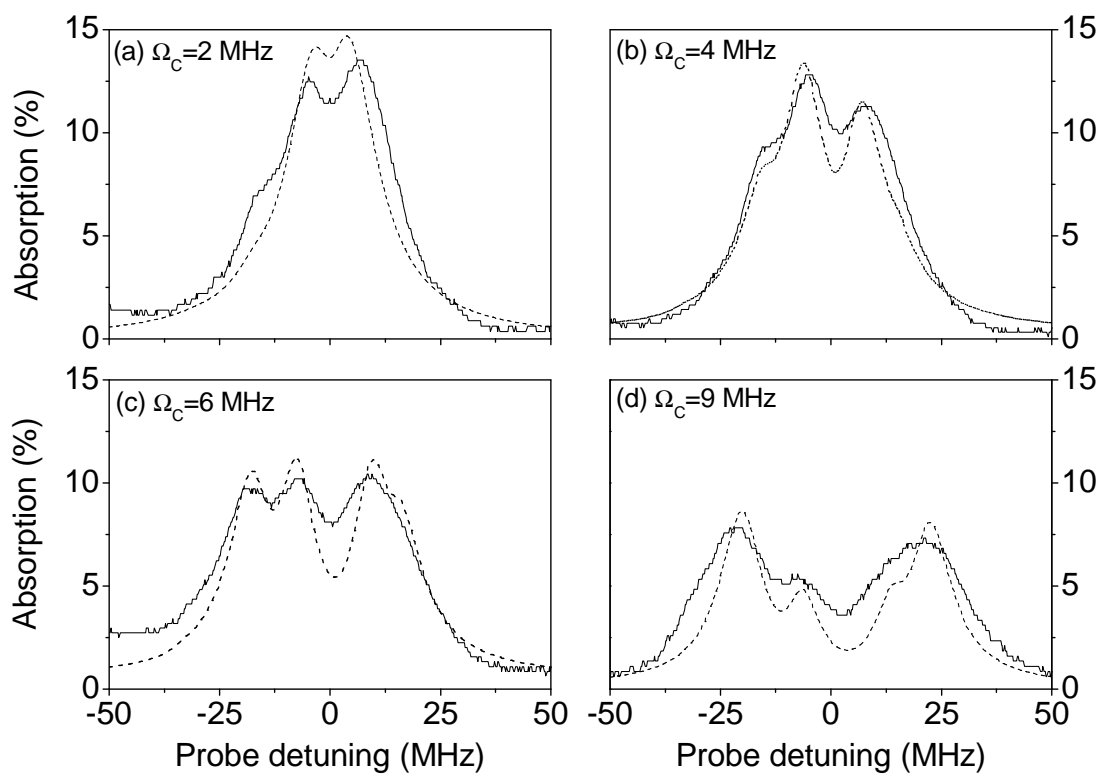


Fig. 5 (J. Wang et al)